

Loss of Phase of Collapsing Beams

Bonggu Shim,^{*} Samuel E. Schrauth, and Alexander L. Gaeta[†]

School of Applied and Engineering Physics, Cornell University, Ithaca, New York 14853, USA

Moran Klein and Gadi Fibich[‡]

Department of Applied Mathematics, Tel Aviv University, Tel Aviv 69978, Israel

(Received 28 May 2011; published 26 January 2012)

We experimentally investigate the phase of an optical field after it has undergone wave collapse. We confirm the theoretical prediction that it acquires a large cumulative nonlinear phase shift that is highly sensitive to small fluctuations of the laser input power. This results in an effective postcollapse “loss of phase,” whereby the phase of the transmitted beam shows a significant increase in sensitivity to the input fluctuations of the pulse energy. We also investigate interactions between two beams that each undergoes collapse and observe large fluctuations in the output mode profiles, which are due to the postcollapse loss of their relative phase difference. Such effects should occur in all systems that exhibit wave collapse.

DOI: 10.1103/PhysRevLett.108.043902

PACS numbers: 42.65.Tg, 42.65.Jx, 42.65.Sf

The phenomenon of wave collapse is universal in various fields of physics such as nonlinear optics, Bose-Einstein condensation, hydrodynamics, and solid-state and plasma physics [1]. When a high-power laser beam propagates in transparent media, self-focusing occurs at input powers above a certain critical power P_{cr} , and the beam undergoes beam collapse. Since the first demonstration of beam collapse and subsequent self-trapping in Kerr media [2,3], its dynamics has attracted significant attention due to the complex and universal phenomena associated with the process. As the intensity of the collapsing beam increases, other nonlinear mechanisms such as plasma formation and multiphoton absorption can occur and counterbalance self-focusing. For propagation in air, the beam can be confined over distances from several meters to a few km, which is known as laser filamentation [4–11]. During the process of collapse and filament formation, self-phase modulation combined with optical shock formation [12] can generate extremely broad spectra which have been termed supercontinuum generation (SCG) [13], and this can be applied to pulse compression to durations as short as a few cycles [14] and to new sources for spectroscopy and remote sensing [15]. Other phenomena that accompany beam collapse and filamentation include pulse splitting [16,17], conical emission [6], and THz radiation [18].

For laser powers much greater than P_{cr} , the collapsing beam breaks up into multiple filaments in which the power in each filament is P_{cr} [5]. Various groups have experimentally investigated the spatial dynamics of multiple filaments and demonstrated mutual interactions that exhibited fusion and competition [19,20]. Although it is difficult to control multifilamentation (MF) patterns since they are initiated by random noise of the laser beam [4], several groups have performed experiments to control the MF using methods such as masks, beam shaping into elliptical

beams, and pinholes [21–23]. Another related area of interest is the control of two filaments by adjusting the time delay and the relative phase (subwavelength time delay). For the control experiments over tens and hundreds of fs time scales, the molecular quantum wakes induced by an intense pump (filament) have been used to control the position and the intensity of a probe (filament) [24,25]. For the case of phase control of the input pulses, it has been theoretically shown [26,27] that two light filaments in air can be phase controlled so that they can show interactions similar to soliton interactions [28]. Ishaaya *et al.* [29] experimentally observed fusion, repulsion, and energy exchange between two parallel collapsing beams in solids, and Shim *et al.* [30] demonstrated the similar effects in air and furthermore showed that spiral motion occurs when they intersect at different planes.

In a recent theoretical study [31], it was shown that a collapsing beam can accumulate a large ($\gg 2\pi$) nonlinear phase shift, and this phase shift is extremely sensitive to small fluctuations of the initial laser power. This effect has been termed “loss of phase,” since the phase of a laser pulse after collapse becomes stochastic, due to small fluctuations in pulse energy. The loss of phase was theoretically predicted to lead to random interference between 2 or more postcollapse interacting filaments [31,32], as has been observed in numerical simulations [33,34]. These results suggest that phase-controlled interactions between high-power beams and/or filaments can be robust for pre-collapse interacting beams, but not for postcollapse ones.

In this Letter, we demonstrate experimentally the loss-of-phase effect with collapsing laser pulses. Almost all studies for the collapse dynamics have focused on the effects on the intensity, and our work represents, to the best of our knowledge, the first experimental study of the phase of a beam that has undergone collapse and the first theoretical explanation for the turbulent behavior that

was previously observed for pulses that contain multiple filaments [33,34]. We show via interferometric measurement that the loss of phase occurs for a single beam and measure the shot-to-shot fluctuations of the phase. In a second set of experiments, we investigate the implication of this effect by interfering two beams that have undergone collapse and show that the large fluctuations occur in the resulting mutual interaction. Both measurements show that as we increase the input beam power, small fluctuations in the laser input power cause a change in the beam phase so that the interaction exhibits significant fluctuations [33,34]. The loss of phase places a severe limitation on the possibility to control the interactions between propagating filaments and is highly relevant to the understanding of the high sensitivity of the MF patterns to the initial beam power.

To understand the phase behavior of collapsing beams, we simulate nonlinear pulse propagation in a Kerr medium using the two-dimensional nonlinear Schrödinger equation in normalized units,

$$\frac{\partial \psi}{\partial z} = i \left(\frac{\partial^2 \psi}{\partial x^2} + \frac{\partial^2 \psi}{\partial y^2} \right) + i |\psi|^2 \psi - i \epsilon |\psi|^4 \psi, \quad (1)$$

where ψ is the complex amplitude of the electric field normalized by the electric field of the initial beam, z is the propagation distance normalized by the diffraction length of the initial beam, and x and y are the transverse coordinates normalized by the initial field radius ($1/e$). The terms on the right-hand side of the equation represent diffraction, Kerr-nonlinearity, and higher-order Kerr nonlinearity as nonlinear saturation [35–38], respectively. Here the nonlinear saturation term is phenomenological and has been added to arrest beam collapse and allow propagation past the collapse point. Figure 1(a) shows the calculated on-axis accumulated phase at $z = 0.85$, which is beyond the initial collapse, as a function of the input power P with $\epsilon = 5 \times 10^{-4}$. As P/P_{cr} varies between 1.275 and 1.377, the on-axis accumulated phase changes by as much as 2π . Here for $P/P_{\text{cr}} = 1.275$ (1.377), the first collapse occurs at $z = 0.43$ (0.36). In other simulations, which are not shown, we see that as z increases, the phase change within the same power interval also increases. In other words, we observe significant changes in the phase at long propagation distances since the phase sensitivity to small changes in the initial condition increases with z . In Fig. 1(b) we plot the

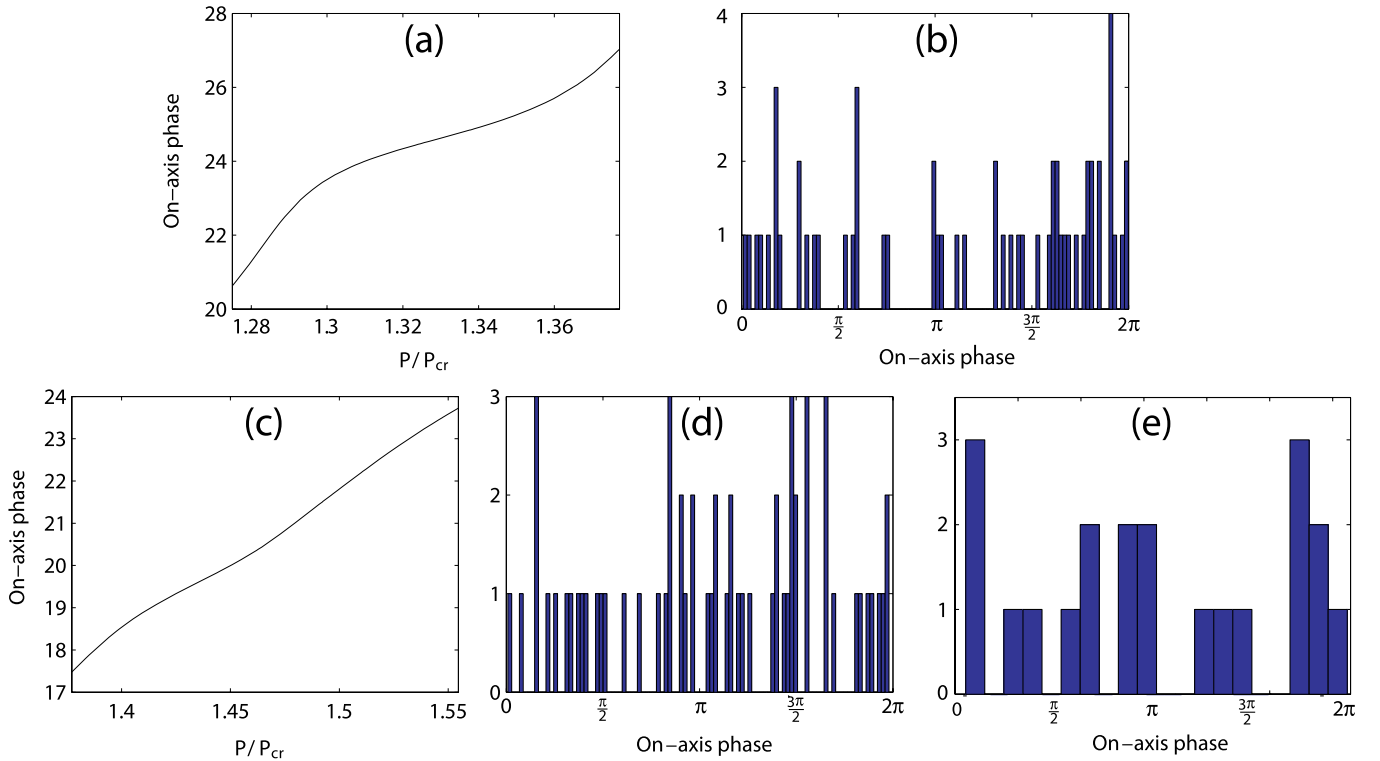


FIG. 1 (color online). (a) On-axis accumulated phase at $z = 0.85$ as a function of P/P_{cr} between 1.275 and 1.377 with higher-order Kerr nonlinearity. Here we assume $\epsilon = 5 \times 10^{-4}$. (b) Histogram of the on-axis phase at $z = 0.85$ for 56 simulations with higher-order Kerr nonlinearity when P/P_{cr} is uniformly distributed between 1.275 and 1.377. (c) On-axis accumulated phase at $z = 1.4$ as a function of P/P_{cr} between 1.38 and 1.55 with plasma defocusing. Here we use $\epsilon = 0.3 \times 10^{-8}$. (d) Histogram of the on-axis phase at $z = 1.4$ for 62 simulations with plasma defocusing when P/P_{cr} is uniformly distributed between 1.38 and 1.55. (e) Histogram of the on-axis phase of collapsing beams in water after 24 cm propagation for 21 simulations when the input beam power is uniformly distributed between 240 and 260 MW.

noncumulative phase at $z = 0.85$ for 56 realizations when P/P_{cr} is uniformly distributed between 1.275 and 1.377, and we observe that the phase fluctuates over the interval $[0, 2\pi]$ as the beam propagates through the collapse region. We observed a similar behavior with other forms of nonlinear saturation terms. For example, if we consider plasma defocusing in water as nonlinear saturation with the term $-i\epsilon|\psi|^{10}\psi$ (see Ref. [30]) instead of the higher-order Kerr term, the similar loss-of-phase effect occurs as is shown Figs. 1(c) and 1(d), too. Indeed, because the loss of phase occurs through the collapse region, it is a universal phenomenon which is independent of the collapse-arresting mechanism (nonlinear saturation, plasma, etc.). We have also performed simulations with the full nonlinear envelope equation taking into account space-time focusing, self-steepening, multiphoton absorption, and plasma [Fig. 1(e)]. We choose 21 different powers in an interval of 240 and 260 MW incorporating our experimental conditions which are described later, and the phase at on-axis maxima clearly shows the loss-of-phase effect.

To investigate experimentally this prediction, we perform Mach-Zehnder type interferometry measurements. In the experiments, Ti:sapphire laser pulses (10 Hz repetition rate, 50-fs FWHM, $\leq 0.5\%$ rms energy fluctuation) centered at 800 nm from a regenerative amplifier pass through a vacuum spatial filter to improve mode profiles. After dividing the input beam using a beam splitter (BS), one beam (signal) passes through a 24-cm distilled water cell, and the other beam (reference) propagates in free space (air). Two beams are then combined at another BS, attenuated by neutral density (ND) filters, and are imaged at the exit of the water cell using a $f/3$ achromat lens onto a 12-bit charge-coupled device (CCD) camera. The output intensity profiles are recorded in a single shot which is a

measure of the phase sensitivity induced by the nonlinear interaction of the signal through the water cell. The diameter of each input beam is approximately 1 mm. Based on single-shot autocorrelation measurements, the weak, non-collapsing signal pulse passing through the water cell broadens to approximately 300 fs due to water dispersion. Significant temporal changes such as pulse splitting are not observed for the range of energies studied. We maintain the same linear polarizations between the two beams and place a motorized delay stage in the reference arm to control time delays with subwavelength resolution. Figure 2 shows the measured on-axis phase ϕ which is given by $\phi = \cos^{-1}[(I - I_r - I_s)/2\sqrt{I_r I_s}]$, where I , I_r , and I_s are the on-axis intensities of the interferometric profile, and the reference and signal beams, respectively. Images of a 100-shot-average of the signal and reference beams are at the bottom for different peak input powers. For $P = 80$ MW [Fig. 2(a)], the signal beam does not collapse inside of the 24-cm water cell (see the signal beam figure at the bottom), and fluctuations of intensity profiles and phases are negligible. However, fluctuations in the phase appear as the probe beam collapses for $P = 240$ MW and larger fluctuations are observed at higher power ($P = 280$ MW). Although we attempted to reset the initial phase to account for the nonlinear phase shift and maximize the on-axis intensity of the interferometric images when we increased the input beam power, the loss-of-phase effect at higher powers prevents precise determination of this optimal phase which results in a shift in average phase value for different powers. Because of the large difference of pulse durations between the reference (50 fs) and signal (300 fs) beams combined with a uncompensated chirp, the phase sensitivity decreases and the extracted phase from interferometry is near $\pi/2$ (no interaction). In addition, a

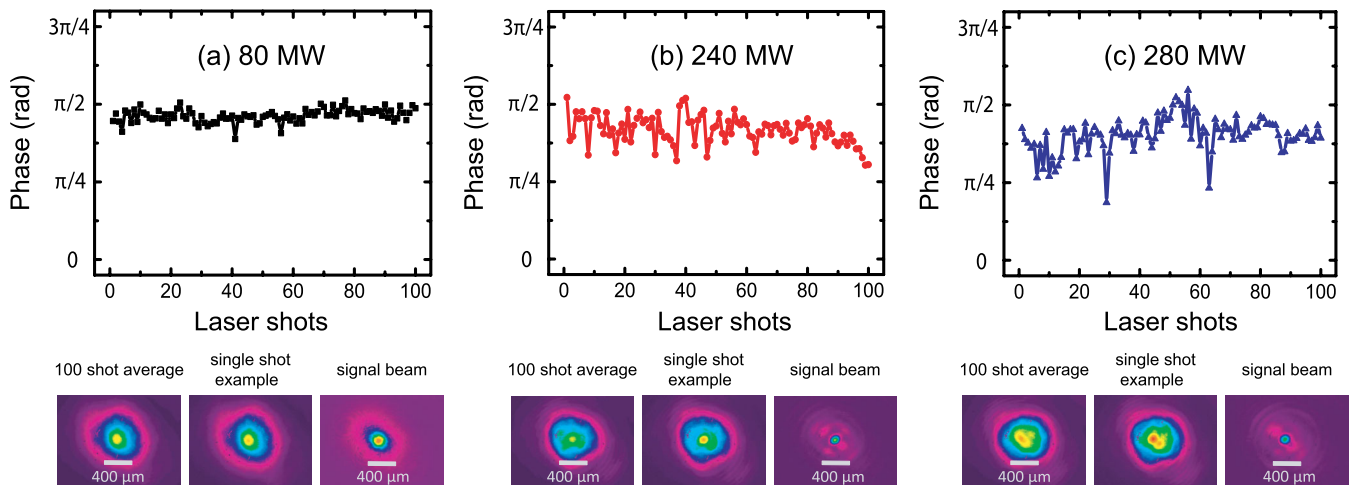


FIG. 2 (color online). Measured on-axis phase for 100 consecutive laser shots from the Mach-Zehnder type interferometry for different peak input powers [$P = (a)80$ MW, (b) 240 MW, and (c) 280 MW]. The 100-shot average interferometry images, the images of typical single-shot examples, and the signal images are shown at the bottom. The signal beam passes through the water cell, experiencing self-focusing, and the reference beam propagates in free space. Here both beams are linearly polarized.

complete loss of phase should occur in the limit as the collapse-arresting mechanisms vanish such that the collapse point is singular. The signal beam images for $P = 240$ and 280 MW show symmetric profiles [2,39] with nearly the same sizes, which indicates the formation of laser filaments due to the balance of self-focusing and nonlinear mechanisms such as MPA and plasma defocusing.

The loss-of-phase phenomenon implies that the interactions between postcollapse beams can become chaotic [31,32]. For example, Ref. [31] performed simulations of two in-phase intersecting beams that undergo individual collapses and show that very slight changes in the relative powers of the two beams lead to dramatic changes in the interaction pattern of postcollapse beams, due to this loss of the relative phase. We experimentally investigate this interacting beam geometry with two crossing beams at nominally the same peak powers. The beams are sent into the 24-cm water cell at a 0.2° crossing angle such that they spatially combine near the output face of the water cell. The beams pass through a quarter-wave plate before the cell to allow for the use of either linear or circular polarizations. In our experiment we observe that the pointing stability of beams with circular polarizations shows little difference between low-power and high-power beams even though beam wander with linear polarizations is more pronounced for high-power collapsing beams [40,41]. Figure 3 shows seven consecutive, single-shot images at the output face of the 24-cm water cell with circular polarizations. The background fringe patterns are due to the small converging angle between the beams. When we set the relative phase to zero for relatively low-power beams ($P = 160$ MW), the intensity profiles

show little fluctuations as is shown in Fig. 3(a). However, as we increase the input beam power ($P = 240$ and 280 MW), each beam collapses and evolves into a circularly symmetric Townes profile [2,39] with $150\text{-}\mu\text{m}$ diameters inside the water cell [see the single-beam figures of Figs. 3(b) and 3(c)]. For $P = 240$ MW, we observe (partial) fusion with shot-to-shot fluctuations in the shapes and peak intensities of the images due to the loss-of-phase effect. For $P = 280$ MW, the shot-to-shot fluctuations are increased due to the larger effect of the loss-of-phase mechanism such that even repulsion is observed [see the first and third figures of Fig. 3(c)]. The measurement with linear polarizations shows similar, power-dependent effects.

We also perform an experiment with two parallel beam geometry [29,30] to explore the effect of this loss of phase can have on interacting filaments. Although beam interactions start to occur before collapse for the parallel case, two high-power beams with an initial π phase difference can individually collapse due to repulsion and thus the loss of phase should still occur after collapse. Figure 4(a) shows that the π phase difference is well maintained for $P = 160$ MW. However, as we increase the input power ($P = 280$ MW), the output intensity profiles show significant fluctuations due to the postcollapse loss of phase [Fig. 4(b)].

In conclusion, we theoretically investigate and experimentally demonstrate the loss of phase for high-power collapsing beams in a Kerr medium. This loss of phase results from the high sensitivity of the accumulated nonlinear phase shift through the collapse point to the input pulse power. Both the interferometric and the two-beam interaction measurements show that small fluctuations in

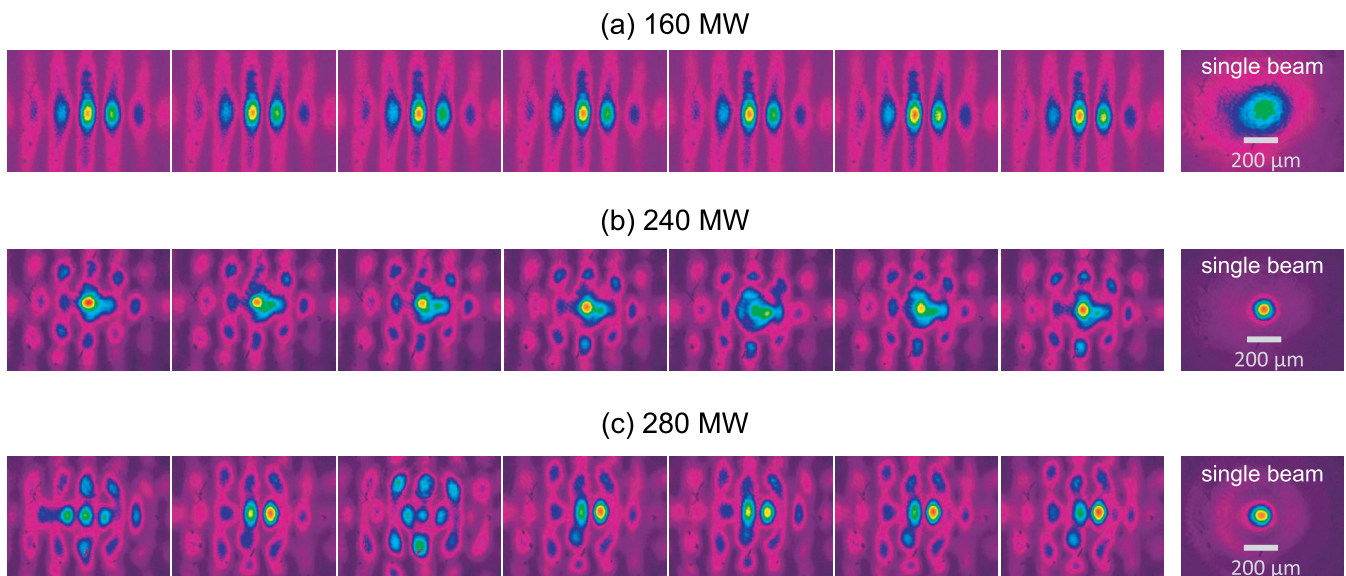


FIG. 3 (color online). Seven consecutive single-shot images of two crossing beams with the initial zero phase at the output face of a 24-cm long water cell for (a) 160 MW, (b) 240 MW, and (c) 280 MW peak input powers. The last figures for each power show single-beam mode images at the output face. Here both beams are circularly polarized.

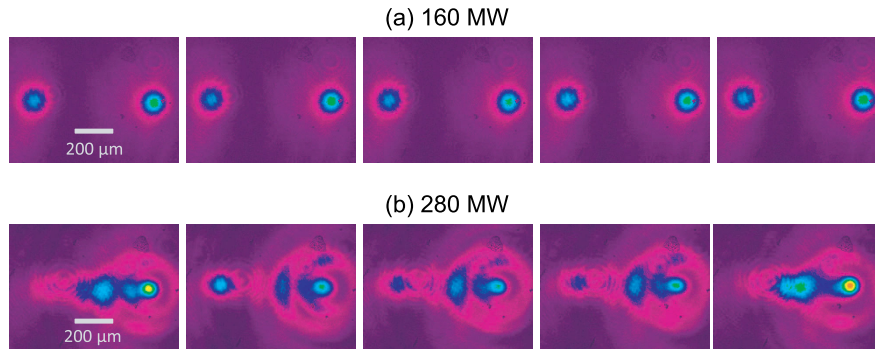


FIG. 4 (color online). Five consecutive single-shot images of two parallel beams with the initial π phase at the output face of a 24-cm long water cell for (a) 160 MW and (b) 280 MW peak input powers. Here both beams are circularly polarized.

the laser input power can cause significant changes in the beam phase, so that postcollapse interactions can exhibit significant sensitivity to the input fluctuations. We note that two previous experiments [29,30] demonstrated stable phase-controlled interactions between two collapsing beams and filaments in air. In those experiments, however, the interactions occurred before the beams collapsed. Thus, phase-controlled beam interactions are only possible if the beams interact before undergoing collapse.

This research was supported by AFOSR and ARO and partially supported by Grant No. 2006-262 from the United States–Israel Binational Science Foundation (BSF), Jerusalem, Israel.

*bgs43@cornell.edu

†a.gaeta@cornell.edu

‡fibich@math.tau.ac.il

- [1] See, for example, P. A. Robinson, *Rev. Mod. Phys.* **69**, 507 (1997).
- [2] R. Y. Chiao, E. Garmire, and C. H. Townes, *Phys. Rev. Lett.* **13**, 479 (1964).
- [3] V. I. Talanov, *JETP Lett.* **2**, 138 (1965).
- [4] V. I. Bespalov and V. I. Talanov, *JETP Lett.* **3**, 307 (1966).
- [5] A. Braun *et al.*, *Opt. Lett.* **20**, 73 (1995).
- [6] E. T. J. Nibbering *et al.*, *Opt. Lett.* **21**, 62 (1996).
- [7] A. Brodeur *et al.*, *Opt. Lett.* **22**, 304 (1997).
- [8] S. L. Chin *et al.*, *Can. J. Phys.* **83**, 863 (2005).
- [9] A. Couairon and A. Mysyrowicz, *Phys. Rep.* **441**, 47 (2007).
- [10] L. Bergé *et al.*, *Rep. Prog. Phys.* **70**, 1633 (2007).
- [11] J. Kasparian and J.-P. Wolf, *Opt. Express* **16**, 466 (2008).
- [12] A. L. Gaeta, *Phys. Rev. Lett.* **84**, 3582 (2000); *Science* **301**, 54 (2003).
- [13] *The Supercontinuum Laser Source*, edited by A. A. Alfano (Springer, New York, 1989).
- [14] C. P. Hauri *et al.*, *Appl. Phys. B* **79**, 673 (2004).
- [15] J. Kasparian *et al.*, *Science* **301**, 61 (2003), and references therein.
- [16] J. K. Ranka, R. W. Schirmer, and A. L. Gaeta, *Phys. Rev. Lett.* **77**, 3783 (1996).
- [17] S. A. Diddams *et al.*, *Opt. Lett.* **23**, 379 (1998).
- [18] C. D'Amico *et al.*, *Phys. Rev. Lett.* **98**, 235002 (2007).
- [19] S. Tzortzakis *et al.*, *Phys. Rev. Lett.* **86**, 5470 (2001).
- [20] S. A. Hosseini *et al.*, *Phys. Rev. A* **70**, 033802 (2004).
- [21] G. Méchain *et al.*, *Phys. Rev. Lett.* **93**, 035003 (2004). Here we believe that the spatial separations between mask holes are relatively large such that the phase relation and/or interactions between filaments are negligible.
- [22] A. Dubietis *et al.*, *Opt. Lett.* **29**, 1126 (2004); G. Fibich *et al.*, *Opt. Lett.* **29**, 1772 (2004); T. D. Grow and A. L. Gaeta, *Opt. Express* **13**, 4594 (2005).
- [23] Z. Hao *et al.*, *Opt. Express* **15**, 16 102 (2007).
- [24] S. Varma, Y.-H. Chen, and H. M. Milchberg, *Phys. Rev. Lett.* **101**, 205001 (2008).
- [25] F. Calegari *et al.*, *Phys. Rev. Lett.* **100**, 123006 (2008).
- [26] L. Bergé *et al.*, *J. Opt. Soc. Am. B* **14**, 2550 (1997).
- [27] T.-T. Xi, X. Lu, and J. Zhang, *Phys. Rev. Lett.* **96**, 025003 (2006).
- [28] G. I. Stegeman and M. Segev, *Science* **286**, 1518 (1999), and references therein.
- [29] A. A. Ishaaya *et al.*, *Phys. Rev. A* **75**, 023813 (2007).
- [30] B. Shim *et al.*, *Phys. Rev. A* **81**, 061803(R) (2010).
- [31] G. Fibich and M. Klein, *Nonlinearity* **24**, 2003 (2011).
- [32] F. Merle, *Commun. Pure Appl. Math.* **45**, 203 (1992).
- [33] M. Mlejnek *et al.*, *Phys. Rev. Lett.* **83**, 2938 (1999).
- [34] L. Bergé *et al.*, *Phys. Rev. Lett.* **92**, 225002 (2004).
- [35] P. Béjot *et al.*, *Phys. Rev. Lett.* **104**, 103903 (2010).
- [36] C. Brée, A. Demircan, and G. Steinmeyer, *Phys. Rev. Lett.* **106**, 183902 (2011).
- [37] P. Béjot *et al.*, *Phys. Rev. Lett.* **106**, 243902 (2011).
- [38] D. Novoa, H. Michinel, and D. Tommasini, *Phys. Rev. Lett.* **105**, 203904 (2010).
- [39] K. D. Moll, A. L. Gaeta, and G. Fibich, *Phys. Rev. Lett.* **90**, 203902 (2003).
- [40] A. Trisorio and C. P. Hauri, *Opt. Lett.* **32**, 1650 (2007).
- [41] According to the pointing stability analysis over 300 shots, the standard deviations of centroid positions for the circularly polarized beams are $\Delta x(\Delta y) = 6.04 \mu\text{m}$ ($5.23 \mu\text{m}$) for 160 MW, $\Delta x(\Delta y) = 3.80 \mu\text{m}$ ($4.58 \mu\text{m}$) for 240 MW, and $\Delta x(\Delta y) = 3.89 \mu\text{m}$ ($4.71 \mu\text{m}$) for 280 MW.